Lecture 13

Constraints on Melt Models Arising From Disequilibrium in the Th-U Decay System

(for reference: see Uranium-Series Geochemistry, volume 52 of Reviews in Mineralogy and Geochemistry (Bourdon, Henderson, Lundstrom, and Turner, editors))

1. The Decay of a Radioactive Isotope

For a radioactive isotope N, we can measure disintegrations/time, i.e., $\dfrac{dN}{dt} = -\lambda N$

where λ = the decay constant = $0.693t_{1/2}$, $t_{1/2}$ = half-life and N is the number of radioactive atoms.

(λN) is known as "activity". Note: (a) This activity is typically indicated by parentheses (^{232}Th) as opposed to $[^{232}Th]$ which designates atomic abundance. (b) Activity as used in radioactive decay is not related to the activity commonly used in thermodynamics.

We can integrate: $\dfrac{dN}{dt} = -\lambda N$ to get $ln\ N = -\lambda t + constant$

At t = o, N = N_o

So C = $ln\ N_o$

$ln\ (N/N_o) = -\lambda t$

$N = N_o e^{-\lambda t}$ (this is the basic equation for radioactive decay).

The definition of half-life $t_{1/2}$, is:

$\dfrac{N}{N_o} = \dfrac{1}{2} = e^{-\lambda t_{1/2}}$

$-ln\ 2 = -\lambda t_{1/2}$

so $t_{1/2} = \dfrac{0.693}{\lambda}$

2. The Concept of Secular Equilibrium

Consider the decay of radioactive nuclide "N" to a daughter nuclide "M" which is itself radioactive. The number of atoms of the daughter nuclide can be calculated from the radioactive decay law. Since daughter nuclides (M) are formed each time parent nuclides (N) decay, the rate of production of the daughter nuclide, $(dM/dt)_{production}$, is just equal to the negative of the decay rate of the parent, dN/dt. As soon as some daughter nuclei have been produced, their decay begins at a rate given by $(dM/dt)_{decay}$. The net growth rate for the daughter nuclide, $(dM/dt)_{net}$, is equal to the sum of the production and decay rates, i.e.,

$$\left(\frac{dM}{dt}\right)_{net} = \left(\frac{dM}{dt}\right)_{production} + \left(\frac{dM}{dt}\right)_{decay}$$

The production and decay rates can be written as $\lambda_N N$ and $-\lambda_M M$, so that

$$\left(\frac{dM}{dt}\right)_{net} = \lambda_N N - \lambda_M M$$

Using $N = N_o e^{-\lambda t}$ and substituting for N we find that

$$\left(\frac{dM}{dt}\right)_{net} = \lambda_N N_o e^{-\lambda_N t} - \lambda_M M \quad .$$

This equation can be rearranged and integrated to give:

$$M = \frac{\lambda_N}{(\lambda_M - \lambda_N)} N_o (e^{-\lambda_N t} - e^{-\lambda_M t}) + M_o e^{-\lambda_M t}$$

Where M is the number of daughter atoms at any time t, N_o is the number of parent atoms at time t = 0, and M_o is the number of daughter atoms at time t = 0. If at t = 0 only the pure parent nuclide is present, then M_o = 0.

3. The Decay Series of U and Th Isotopes

Both U and Th have isotopes with relatively long half-lifes; consequently, $^{232}_{90}\text{Th}$, $^{235}_{92}\text{U}$ and $^{238}_{92}\text{U}$ occur in all natural materials (Figure 42).

Isotope	Abundance (%)	Half-life (years)	Decay Constant (y^{-1})
^{238}U	99.2743	4.468 x 10^9	1.55125 x 10^{-10}
^{235}U	0.7200	0.7038 x 10^9	9.8485 x 10^{-10}
^{232}Th	100.00	14.010 x 10^9	4.9475 x 10^{-11}

Figure 42. Abundances, half-lifes and radioactive decay constants of relatively long-lived, hence naturally occurring, isotopes of Uranium and Thorium.

In this discussion we are particularly interested in the decay of ^{238}U which ultimately decays to ^{206}Pb via a complex series (chain) of decay events (Figure 43). An important aspect of this radioactive decay chain is that the half-life of ^{238}U is much longer than the half-life of each daughter nuclide, e.g., $^{238}_{90}\text{U} \rightarrow ^{234}_{90}\text{Th} + ^4_2\text{He}$ (i.e., an alpha particle) has a half-life of 4.47 x 10^9 years but $^{234}_{90}\text{Th} \rightarrow ^{234}_{91}\text{Pa} + \beta$ has a half-life of only 24.1 days.

In this case the previous equation:

$$M = \frac{\lambda_N}{(\lambda_M - \lambda_N)} N_o (e^{-\lambda_N t} - e^{-\lambda_M t}) + M_o e^{-\lambda_M t}$$

can be simplified because $\lambda_M \gg \lambda_N$, so that $e^{-\lambda_M t}$ is negligible compared to $e^{-\lambda_N t}$ and $(\lambda_M - \lambda_N) \sim \lambda_M$. Assuming that at $t = 0$, $M_o = 0$ this equation becomes:

$$M = \frac{(\lambda_N)}{(\lambda_M)} N_o e^{-\lambda_N t} \quad .$$

Since $N = N_o e^{-\lambda t}$ -lt this equation further simplifies to

$$\lambda_M M = \lambda_N N \quad .$$

Thus, the disintegration rate of the daughter nuclide equals the disintegration rate of the parent. This circumstance is known as "secular equilibrium" and occurs only after sufficient time for growth of the daughter activity. Specifically, it can be shown that starting with the pure parent, the daughter activity will have reached half its equilibrium value after a time lapse equal to 1 half-life of the daughter and secular equilibrium will be essentially attained after 5 half-lifes of the daughter nuclide. It is important to realize that the half-life of the daughter nuclide controls the approach to secular equilibrium.

When secular equilibrium is established and the relatively long-lived parental nuclide decays, i.e. ^{238}U, each of the succeeding radioactive nuclides decays, e.g. decay of a ^{238}U nuclide is accompanied by decay of ^{234}Th, ^{234}Pa, ^{234}U, ^{230}Th, etc. with the final step being formation of a stable nuclide of ^{206}Pb (Figure 43). This coordinated sequence of events is akin to a line of soldiers marching in step.

There are many earth science applications of measuring departures from and return to secular equilibrium. We focus on (^{238}U/^{230}Th) activity ratios because an assessment of this ratio in young lavas provides constraints on the melting process.

Z

85   90

206 Pb — Stable

U²³⁸ decay chain
(Principal path)

125

α

210 Po — 138.4 da

β⁻ 210 Bi — 5.0 da

β⁻ 210 Pb — 22 yr

α

130

214 Po — 1.6 x 10⁻⁴ sec

β⁻ 214 Bi — 19.7 min

β⁻ 214 Pb — 26.8 min

α

218 Po — 3.05 min

N 135 α

3.82 da — 222 Rn

α

1,620 yr — 226 Ra

α

7.50 x 10⁴ yr — 230 Th

140 α

2.48 x 10⁵ yr — 234 U

1.18 min — 234m Pa β⁻

24.10 da — 234 Th β⁻

α

145

4.47 x 10⁹ yr — 238 U

:][i fY˙VmˊA =H˙C dYb 7 ci fgYK UfY"

Figure 43.   Radioactive decay chain showing steps in the decay series of ²³⁸U decaying to ²⁰⁶Pb.

5

4. Presentation and Interpretation of ^{238}U/^{230}Pb) Data

Figure 44 shows the expected trends for secular equilibrium defined by the equations when $(^{238}U) = (^{230}Th)$.

:][i fY˙VmA ≠H˙C dYb 7 ci fgYK UfY"
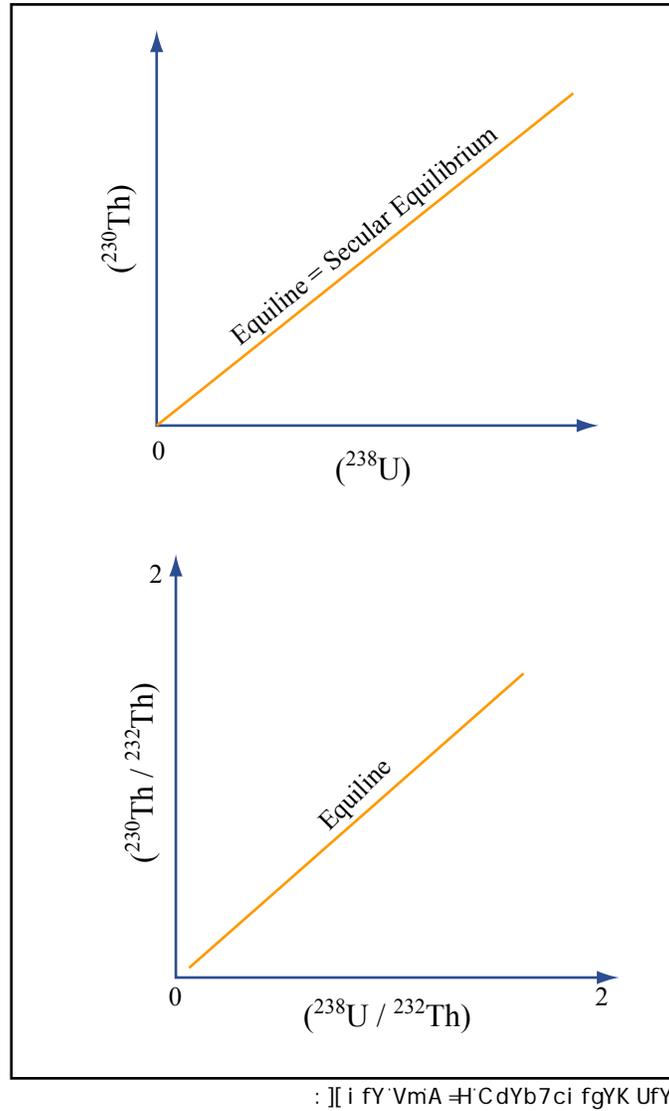
Figure 44. Path of secular equilibrium between (^{238}U) and ^{230}Th). Parentheses indicate activity.
Upper: For chemical systems that have been undisturbed for ~350,000 yrs (~5 times the $t_{1/2}$ of ^{230}Th), we expect samples to be on the equiline which corresponds to secular equilibrium.
Lower: Since it is easier to precisely measure isotopic ratios, rather than number of nuclides, we divide each axis by (^{232}Th). The vertical axis $(^{230}Th/^{232}Th)$ is an isotopic ratio that is not easily changed by geologic processes but because ^{230}Th is unstable its activity changes on timescales of 10^3 years. The horizontal axis $(^{238}U/^{232}Th)$ is an elemental abundance ratio that can be changed by process, e.g., partial melting if D's are different for U and Th, and over long times, 10^9 years, because each isotope has a long but different half-life.
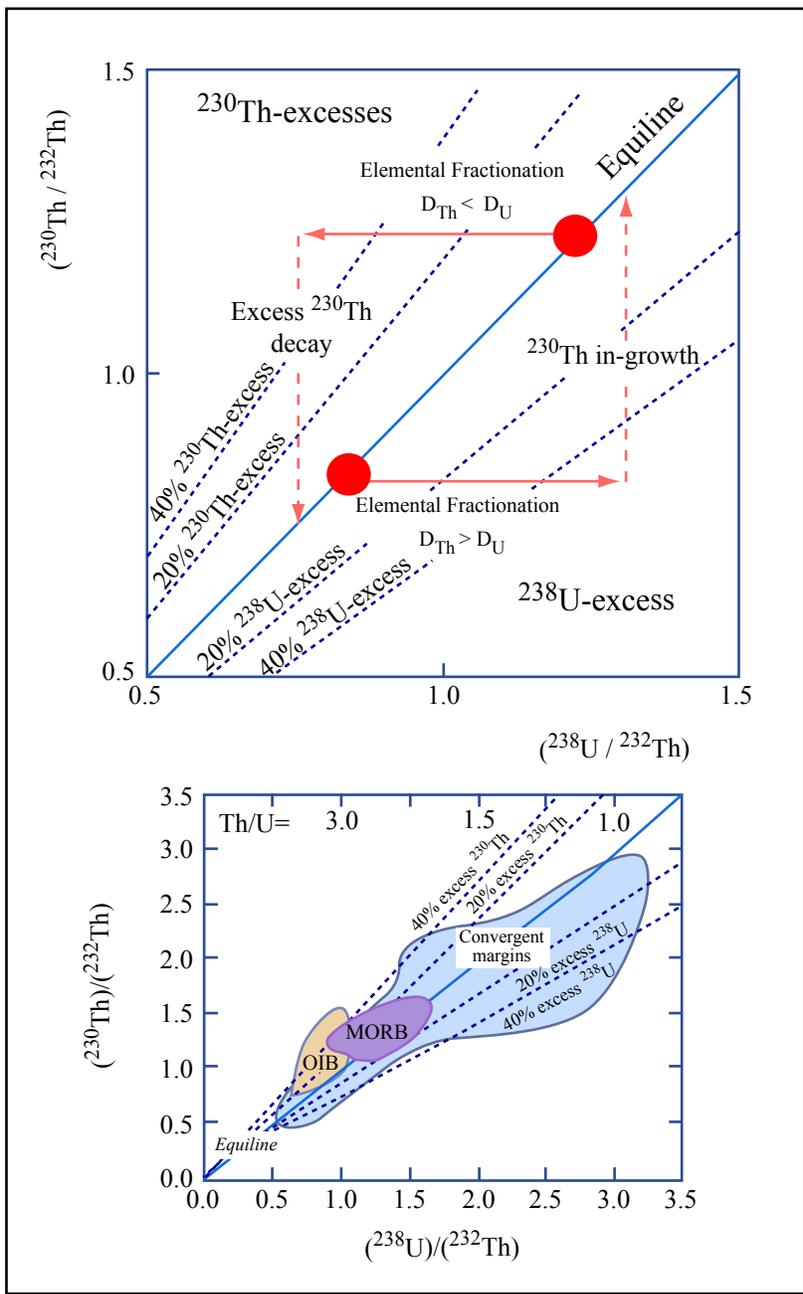
Figure 45. Upper: ^{238}U-^{230}Th systematics illustrated on an equiline diagram. The red circles show source values which are assumed to be in secular equilibrium. Two instantaneous melt events (horizontal solid lines with arrows) change the $(^{238}U/^{232}Th)$ of the melts because $D_{Th}^{s/\ell}$ is not equal to $D_{U}^{s/\ell}$. As a result these melts plot off the equiline. However, with time $(^{230}Th/^{232}Th)$ changes so that the melts return to secular equilibrium (vertical dashed lines with arrows). Also plotted are the loci of secular equilibrium, the equiline (solid diagonal line), and reference degrees of disequilibrium, at $(^{230}Th/^{238}U) = 1.4$ and 1.2, i.e., 40% and 20% ^{230}Th-excesses and $(^{238}U/^{230}U) = 1.4$ and 1.2, i.e., 40% and 20% ^{238}U-excesses (dashed diagonal lines).

Lower: Typical results for $(^{238}U/^{232}Th)$ vs. $(^{230}Th/^{232}Th)$ in young basalts from mid-ocean ridges (MORB), oceanic islands (OIB) and convergent margins (arc) showing that oceanic basalts typically erupt with ^{230}Th excesses in contrast to arc lavas which commonly have ^{238}U excess. Figure is adapted from Lundstrom (2003).

Figure 45 (upper) shows how a system at secular equilibrium, i.e. plotting on the equiline, is perturbed by partial melting. If $D_{Th}^{solid/melt}$ is less than $D_U^{solid/melt}$ the partial melt is preferentially enriched in Th, hence ($^{238}U/^{230}Th$) is decreased in the partial melt as shown by the left pointing arrow; the jargon is that the melt has ^{230}Th excess. Analogously, if $D_{Th}^{solid/melt}$ is greater than $D_U^{solid/melt}$ the partial melt increases in ($^{238}U/^{230}Th$) and has a ^{238}U excess.

Figure 45 (lower) shows that young oceanic basalts are characterized by ^{230}Th excesses, a result commonly attributed to residual garnet, since for garnet $D_{Th} < D_U$ (see Blundy and Wood, 2003). Note that basalts erupted >350,000 years ago will have returned to secular equilibrium and should plot on the equiline.

5. How Much Change in Th/U Can Result From Partial Melting?

The answer to this question depends on the relative values of F (degree of melting) and the (bulk solid)/melt partition coefficients for Th and U. Recall the batch melting equations derived in Lecture 9; that is for element "i"

$$C_i^{\ell}/C_i^o = \frac{1}{F + D_i^{s/\ell}(1-F)} \ .$$

Writing this equation for two elements such as Th and U results in

$$\frac{(C_{Th}/C_U)^{\ell}}{(C_{Th}/C_U)^o} = \frac{F + D_U^{s/\ell}(1-F)}{F + D_{Th}^{s/\ell}(1-F)}$$

which as $F \rightarrow O$ becomes

$$\frac{(C_{Th}/C_U)^{\ell}}{(C_{Th}/C_U)^o} = \frac{D_U^{s/\ell}}{D_{Th}^{s/\ell}}$$

8

Figure 46 shows that significant increase in Th/U in a partial melt of garnet peridotite occurs only when F <1%. This result raised considerable concern because the low (<1%) extent of melting required to explain the Th excess in oceanic basalt is in conflict with inferences based on major element composition that the oceanic crust is formed by 5 to 15% partial melting (e.g., Langmuir et al., 1992).
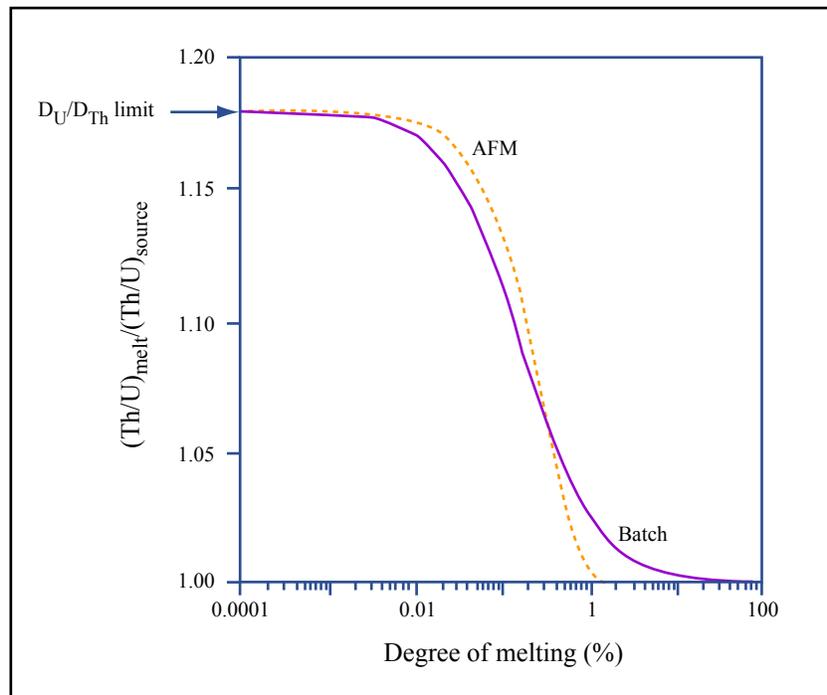
:][i fY˙Vm˙A ꓱH˙C dYb 7 ci fgYK UfY"

Figure 46. Fractionation of (Th/U) ratio in partial melts relative to the initial ratio of the unmelted garnet perdidotite source. Melting curves are shown for equilibrium (batch), solid line, and accumulated fractional melting (AFM) (Shaw, 1970), dashed line. Modal melting is assumed in the calculation, but since the most significant variations occur at low degrees of melting, where consumption of major phases is small, this simplification has little effect when extrapolating to more realistic scenarios. Significant fractionation of Th/U in the melt compared to its source is only achieved at degrees of melting below 1%, and approaches the limit of fractionation, D_U/D_{Th}, at very low degrees of melting.

The garnet peridotite source is assumed to have 10% garnet (gnt) and 10% clinopyroxene (cpx). Partition coefficients of $D_{Th}(cpx) = 0.015$, $D_U(cpx) = 0.01$, $D_{Th}(gnt) = 0.0015$ and $D_U(gnt) = 0.01$ are used. Other major mineral phases make an insignificant contribution to U-Th partitioning. Bulk solid/melt partition coefficients are 0.0016 and 0.00197 for Th and U, respectively. Notably, even in the extreme limit of fractionation, only 17% ^{230}Th-excesses can be generated using these bulk partition coefficients; this is less than observed in many mantle-derived melts (Figure 45). For a review of mineral/melt partition coefficients for Th and U see Blundy and Wood (2003). This figure is adapted from Elliott (1997).

9

6. Can More Complex Melting Models Explain the Significant Observed Th Excess in Oceanic Basalts?

This issue is clearly addressed by Elliott et al. (1997). Because we are considering the behavior of the radioactive isotope ^{230}Th with a relatively short half-life of ~75,000 years, the duration of the melting process is important if it is significant relative to 75,000 years. In Figure 40 (Lecture 12) we considered the concepts of **Continuous Melting** and **Dynamic Melting**. For a stable isotope these two melting models are described by the same equations, but for a radioactive isotope, such as ^{230}Th, the two models lead to different results because the duration of the melting process is important in the **Dynamic Melting** model. For example, if we visualize **Dynamic Melting** as a series of melting steps (Figures 47 and 48), and if $D_{Th}^{bulk\ solid/melt} < D_{U}^{bulk\ solid/melt}$, as expected for garnet peridotite, the residue created in each step has a very high U/Th ratio. As a result during the finite time of the melting process, ^{230}Th ingrows from ^{238}U in order to return to the equiline (Figure 48). Note, however, as melting continues during the upwelling process, i.e. **Dynamic Melting**, the ingrown ^{230}Th will be removed from the residue to the melt, thereby creating more high U/Th residue which will further ingrow more ^{230}Th (Figure 48).

Note that in this melting model U/Th fractionation occurs even when the overall extent of melting is so large that there is no ^{238}U/^{232}Th fractionation. It is essential however, that the melt increments are sufficiently small that ^{238}U/^{230}Th fractionation between the melt and residue can occur.

In summary, the common observation of ^{230}Th excess in oceanic basalts provides constraints in the melting process; i.e., either the extents of melting to create oceanic

basalts are very low, <1%, or the duration of the melting process is important, as it is

in **Dynamic Melting** (Figures 47 and 48).

In addition, $D_{Th}^{bulk\ solid/melt}$ must be less than $D_{U}^{bulk\ solid/melt}$ and this is a

characteristic of garnet (Blundy and Wood, 2003).
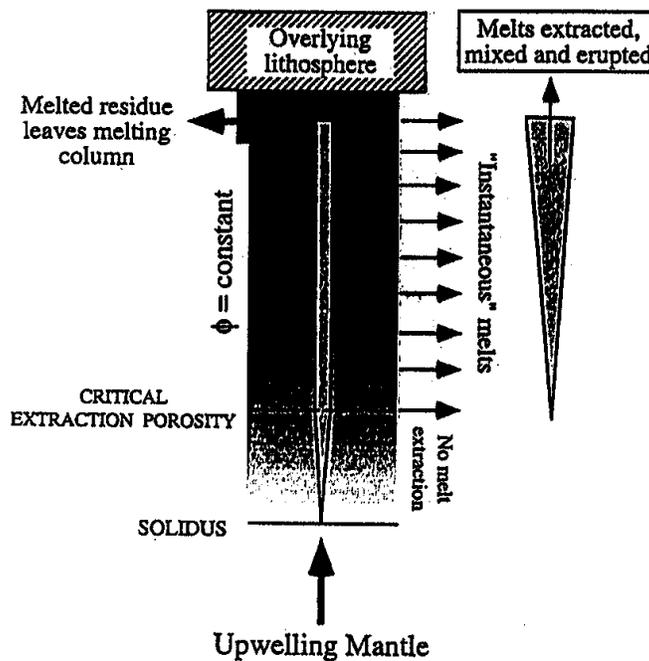
Figure 47. The steady state, one-dimensional Dynamic Melting Process (see Figure 40 and McKenzie, 1985): Mantle upwells, intersects its solidus and melts due to adiabatic decompression until it exits, horizontally, out of the melting regime. Thick arrows indicate direction of mantle movement. No melt is extracted until a critical porosity (ϕ) is reached. After this threshold, each new infinitesimal melt increment (instantaneous melt) generated is extracted to keep the porosity constant. This is shown as a series of discrete events (horizontal arrows). At any point in the melting column, melt and residue are in local equilibrium, but once extracted, melts are assumed to be transported in chemical isolation (disequilibrium transport). Dynamic melting assumes instantaneous transport of melts to the surface. Instantaneous melts produced from all depths of the column are mixed prior to eruption, to form the aggregate, steady state melt. The melting column is shaded according to depletion in compatible element constant (the darker the shading, the more depleted). Lighter shading within the melting column indicates the size of the residual porosity, and the inverted triangle outside the column illustrates the accumulated fraction of extracted instantaneous melts with depth. Figure is from Elliott, 1997.

(a) The effects of the dynamic melting regime on ^{238}U-^{230}Th systematics illustrated using discrete, multiple melting events. Instantaneous melts are shown as squares, and melted residues as small circles.
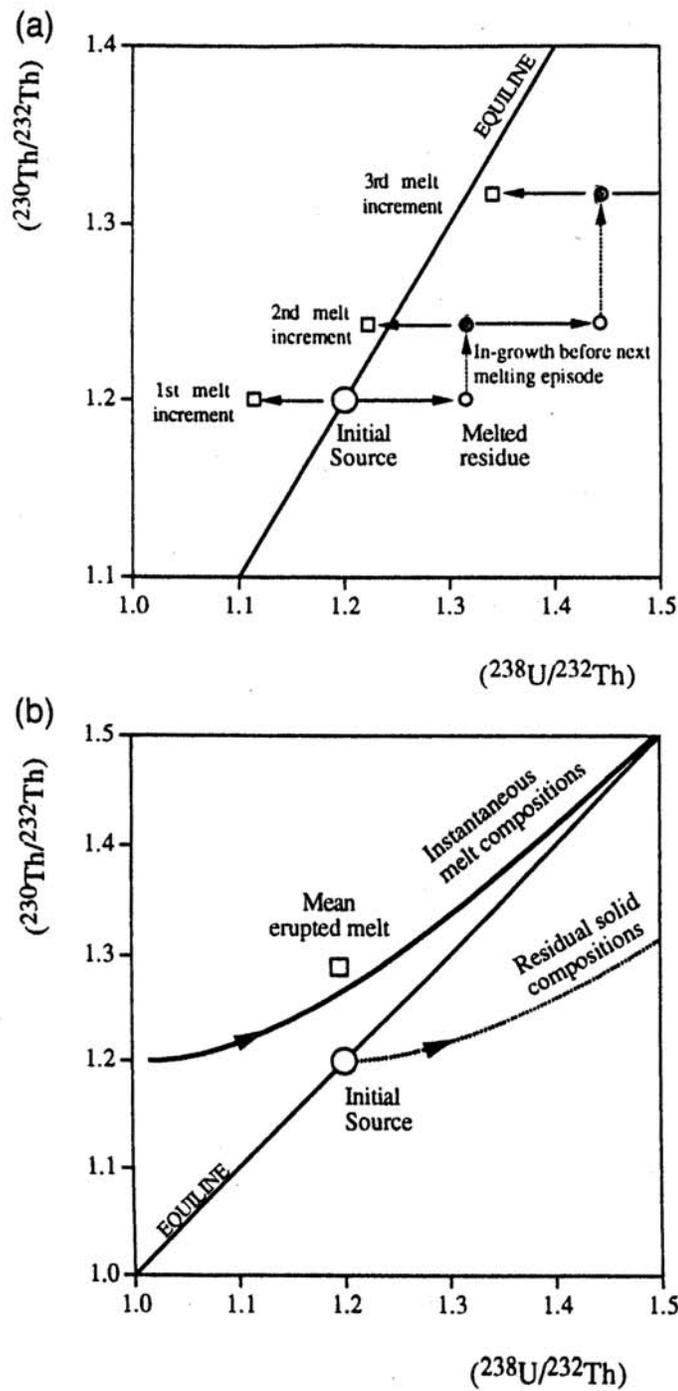
Figure 48. (a) The effects of the dynamic melting regime on ^{238}U-^{230}Th systematics illustrated using discrete, multiple melting events. Instantaneous melts are shown as squares, and melted residues as small circles. The effects of melt fractionation are shown by horizontal arrowed lines, and the passage of time is indicated by dashed vertical arrows that join initial (open circles) and aged (shaded circles) residues. (b) Calculation of the continuous evolution of residual solid and instantaneous melt compositions with increasing degree of melting (or height) in the dynamic melting column. Arrows indicate direction of compositional change with increasing degree of melting. In this example of only 1% total melting, the melting trajectories, extend beyond the edge of the diagram to extreme (^{230}Th/^{232}Th) and (^{238}U/^{232}Th). The instantaneous melt compositions in fact cross the equiline, which does not represent a limiting boundary. The averaged instantaneous melts of the whole melting column, which form the mean erupted melt, is shown as a square. Figure is from Elliott, 1997.

12

12.479 Trace-Element Geochemistry

Spring 2013